DOI:10.1158/0008-5472.CAN-03-4062

Cancer Research

Mechanism of the Pharmacokinetic Interaction between Methotrexate and Benzimidazoles : Potential Role for Breast Cancer Resistance Protein in Clinical Drug-Drug Interactions

Pauline Breedveld, Noam Zelcer, Dick Pluim, et al.

Cancer Res 2004;64:5804-5811. Published online August 16, 2004.

Updated Version Access the most recent version of this article at: doi:10.1158/0008-5472.CAN-03-4062

Cited Articles This article cites 58 articles, 31 of which you can access for free at: http://cancerres.aacrjournals.org/content/64/16/5804.full.html#ref-list-1

Citing Articles This article has been cited by 34 HighWire-hosted articles. Access the articles at: http://cancerres.aacrjournals.org/content/64/16/5804.full.html#related-urls

E-mail alerts Sign up to receive free email-alerts related to this article or journal.

Reprints and Subscriptions To order reprints of this article or to subscribe to the journal, contact the AACR Publications Department at pubs@aacr.org.

Permissions To request permission to re-use all or part of this article, contact the AACR Publications Department at permissions@aacr.org.

Downloaded from cancerres.aacrjournals.org on June 8, 2012
Copyright © 2004 American Association for Cancer Research

DOI:10.1158/0008-5472.CAN-03-4062

[CANCER RESEARCH 64, 5804–5811, August 15, 2004]

Mechanism of the Pharmacokinetic Interaction between Methotrexate and Benzimidazoles: Potential Role for Breast Cancer Resistance Protein in Clinical Drug-Drug Interactions

Pauline Breedveld,[1] Noam Zelcer,[2] Dick Pluim,[1] Özgür Sönmezer,[1] Matthijs M. Tibben,[5] Jos H. Beijnen,[4,5,6] Alfred H. Schinkel,[1] Olaf van Tellingen,[3] Piet Borst,[2] and Jan H. M. Schellens[1,4,6]

Divisions of [1]Experimental Therapy, [2]Molecular Biology, [3]Clinical Chemistry, and [4]Medical Oncology, The Netherlands Cancer Institute, Amsterdam; [5]Department of Pharmacy and Pharmacology, Slotervaart Hospital, Amsterdam; and [6]Faculty of Pharmaceutical Sciences, Utrecht University, Utrecht, the Netherlands

ABSTRACT

The antifolate drug methotrexate (MTX) is transported by breast cancer resistance protein (BCRP; ABCG2) and multidrug resistance-associated protein1–4 (MRP1–4; ABCC1–4). In cancer patients, coadministration of benzimidazoles and MTX can result in profound MTX-induced toxicity coinciding with an increase in the serum concentrations of MTX and its main metabolite 7-hydroxymethotrexate. We hypothesized that benzimidazoles interfere with the clearance of MTX and/or 7-hydroxymethotrexate by inhibition of the ATP-binding cassette drug transporters BCRP and/or MRP2, two transporters known to transport MTX and located in apical membranes of epithelia involved in drug disposition. First, we investigated the mechanism of interaction between benzimidazoles (pantoprazole and omeprazole) and MTX *in vitro* in membrane vesicles from Sf9 cells infected with a baculovirus containing human *BCRP* or human *MRP2* cDNA. In Sf9-BCRP vesicles, pantoprazole and omeprazole inhibited MTX transport (IC_{50} 13 μM and 36 μM, respectively). In Sf9-MRP2 vesicles, pantoprazole did not inhibit MTX transport and at high concentrations (1 mM), it even stimulated MTX transport 1.6-fold. Secondly, we studied the transport of pantoprazole in MDCKII monolayers transfected with mouse *Bcrp1* or human *MRP2*. Pantoprazole was actively transported by Bcrp1 but not by MRP2. Finally, the mechanism of the interaction was studied *in vivo* using *Bcrp1*$^{-/-}$ mice and wild-type mice. Both in wild-type mice pretreated with pantoprazole to inhibit Bcrp1 and in *Bcrp1*$^{-/-}$ mice that lack Bcrp1, the clearance of i.v. MTX was decreased significantly 1.8- to 1.9-fold compared with the clearance of i.v. MTX in wild-type mice. The conclusion is as follows: benzimidazoles differentially affect transport of MTX mediated by BCRP and MRP2. Competition for BCRP may explain the clinical interaction between MTX and benzimidazoles.

INTRODUCTION

Methotrexate (MTX) is an antifolate drug, which is frequently used in the treatment of, *e.g.*, childhood acute leukemia and rheumatoid arthritis. The clinical application of MTX is hampered by the development of drug resistance and the existence of potentially toxic drug-drug interactions with many commonly used drugs.

Resistance to MTX occurs via several mechanisms and can involve amplification or mutation of the target enzyme dihydrofolate reductase, as well as reduced drug uptake by a mutated reduced folate carrier, or alterations in the enzymes involved in MTX polyglutamylation (1–4). In addition, members of the multidrug resistance-associated protein subfamily of ATP-binding cassette-transporters (MRP1–4; ABCC1–4) and breast cancer resistance protein (BCRP; ABCG2) have been shown recently to play a role in MTX resistance and transport *in vitro* (5–13).

Clinically important pharmacokinetic drug-drug interactions exist between (intermittent high-dose or chronic low-dose) MTX and, *e.g.*, nonsteroidal anti-inflammatory drugs, salicylic acid, and probenecid. These interactions may result in bone marrow suppression and acute renal failure (14–17). Takeda *et al.* (18) speculated that hOAT1, hOAT3, hOAT4, and possibly other transporters are involved in these interactions. Furthermore, in cancer patients, interactions have been reported between MTX, its main metabolite 7-hydroxymethotrexate, and the benzimidazoles omeprazole and pantoprazole, resulting in long-lasting extensive myelosuppression associated with systemic infections and severe mucositis (19–21). Omeprazole and pantoprazole inhibit the gastric hydrogen-potassium adenosine triphosphatase (H^+, K^+-ATPase) and are frequently used in the treatment of peptic ulcers, pyrosis, and gastroesophageal reflux disease. Omeprazole was shown to inhibit MTX clearance, resulting in sustained, highly toxic MTX levels (20, 21). Coadministration with pantoprazole resulted in a 70% increase in the serum concentration of the metabolite 7-hydroxymethotrexate (19).

We hypothesized that benzimidazoles interfere with the renal (and possibly hepatic) clearance of MTX and/or 7-hydroxymethotrexate by inhibition of the ATP-binding cassette-transporters BCRP and/or MRP2, two transporters known to transport MTX and located in apical membranes of epithelia involved in drug disposition. To test this hypothesis, we first investigated the mechanism of interaction between benzimidazoles and MTX *in vitro* in membrane vesicles from Sf9 cells infected with baculovirus containing human *BCRP* or *MRP2* cDNA. Secondly, we studied in another drug transport model, *i.e.*, MDCKII cells transfected with mouse *Bcrp1* or human *MRP2*, whether pantoprazole itself is transported by Bcrp1 and/or MRP2. In addition, we studied in the MDCKII-*Bcrp1* monolayers the effect of pantoprazole on the transport of the topoisomerase I inhibitors topotecan and SN38, which are good substrate drugs of BCRP (22, 23). Finally, we investigated the mechanism of the interaction between MTX and benzimidazoles *in vivo* by studying the plasma pharmacokinetics and fecal and urinary excretion of i.v.-administered MTX in *Bcrp1* knockout and wild-type mice with or without coadministration of pantoprazole.

MATERIALS AND METHODS

Chemicals and Reagents. [^{3}H]MTX (5.9 Ci/mmol), [^{3}H]inulin (0.54 Ci/mmol), and inulin[^{14}C]carboxylic acid (6.90 mCi/mmol) were obtained from Amersham (Little Chalfont, United Kingdom). The [^{3}H]$E_2$17βG (40.5 Ci/mmol) was purchased from NEN Life Science Products (Boston, MA). Topotecan (Hycamtin) and [^{14}C]topotecan (56 Ci/mmol) were obtained from Smith-Kline Beecham Pharmaceuticals (King of Prussia, PA). SN38 was a generous gift from Aventis (Vitry sur Seine, Cedex, France). Vials of pantoprazole (Pantozol, 40 mg; Altana Pharma, Zwanenburg, the Netherlands), omeprazole (Losec, 40 mg; AstraZeneca, Zoetermeer, the Netherlands), and MTX (Emthexate PF, 25 mg/ml; Pharmachemie, the Netherlands) were obtained from the pharmacy of The Netherlands Cancer Institute. GF120918 (elacridar) was a generous gift from Glaxo Wellcome (Research Triangle Park, NC), and PSC833 was a kind gift from Dr. M. Lemaire (Novartis, Basel, Switzerland). Creatine phosphate and creatine kinase were obtained from Boehringer Mann-

Received 12/29/03; revised 5/19/04; accepted 6/14/04.

The costs of publication of this article were defrayed in part by the payment of page charges. This article must therefore be hereby marked *advertisement* in accordance with 18 U.S.C. Section 1734 solely to indicate this fact.

Requests for reprints: Jan H. M. Schellens, Department of Medical Oncology, The Netherlands Cancer Institute, Plesmanlaan 121, 1066 CX Amsterdam, the Netherlands. Phone: 31-20-512-2569; Fax: 31-20-512-2572; E-mail: j.schellens@nki.nl.

Downloaded from cancerres.aacrjournals.org on June 8, 2012
Copyright © 2004 American Association for Cancer Research

DOI:10.1158/0008-5472.CAN-03-4062

heim (Almere, the Netherlands), and OE67 filters were from Schleicher and Schuell (Dassel, Germany). All of the other chemicals and reagents were of analytical grade or better and were purchased from Sigma (St. Louis, MO).

Cell Lines. The MDCKII cells were cultured in DMEM supplemented with 10% FCS and 100 units penicillin/streptomycin/ml (24). Cells were grown at 37°C with 5% CO_2 under humidifying conditions. Polarized MDCKII cells stably expressing human *MRP2 (ABCC2*) or murine *Bcrp1* (*ABCG2*) cDNA have been described previously (7, 22, 25). Sf9 insect cells in suspension were grown in Sf-900 II serum-free medium in the absence of serum (Invitrogen). The *MRP2* cDNA and *BCRP* cDNA containing baculoviruses were a kind gift from Balasz Sarkadi (National Institute of Hematology, Budapest, Hungary; Ref. 7).

Protein Analysis and Immunoblotting. Membrane vesicle preparations were diluted in buffer [10 mM KCl, 1.5 mM $MgCl_2$, and 10 mM Tris-HCl (pH 7.4)] supplemented by a cocktail of protease inhibitors used at the concentration recommended by the manufacturer (Roche, Mannheim, Germany). The indicated amount of protein was size-fractionized on a 7.5% SDS polyacrylamide gel and subsequently blotted overnight in a tank blotting system. Multidrug resistance-associated protein2 and BCRP were detected with the monoclonal antibodies M2II5 (1:250) and BXP-21 (1:150), respectively, as described previously (25, 26). Signals were visualized with chemiluminescence (enhanced chemiluminescence; Amersham, United Kingdom).

Preparation of Membrane Vesicles and Vesicular Transport Assays. Membrane vesicles from Sf9 cells were obtained after infection with an *MRP2* or *BCRP* cDNA containing baculovirus at a multiplicity of infection of 1 and were prepared as described previously (27). Vesicular transport assays were performed in buffer consisting of 100 mM KCl and 50 mM HEPES/KOH (pH 7.4) in the presence or absence of 4 mM ATP (28). The time- and concentration-dependent uptake of substrates into membrane vesicles were studied after the rapid filtration method as described previously (29). The ATP-dependent transport was calculated by the difference in transport in the absence or presence of ATP.

Transport Across MDCKII Monolayer. Cells were seeded on microporous polycarbonate membrane filters (Transwell 3414; Costar, Corning, NY) at a density of 1×10^6 cells/well in 2 ml of complete medium. Cells were grown for 3 days with medium replacements every day. Two hours before the start of the experiment, medium on both the apical and the basal sides of the monolayer was replaced with 2 ml of Optimem medium (Life Technologies, Inc. Ltd., Paisley, Scotland) containing the appropriate concentration of transport modulator and also 5 μM PSC833 to inhibit endogenous P-glycoprotein (P-gp) levels or 1 μM GF120918 (elacridar) to inhibit endogenous P-gp and Bcrp1 levels (22). The experiment was started by replacing the preincubation medium on either the apical or the basal side of the cell layer with 2 ml of the similar medium also containing the appropriate concentration of radiolabeled drug and radiolabeled inulin. Inulin was added to check for the intactness of the monolayer. The cells were incubated at 37°C in 5% CO_2, and 50 μl of aliquots were taken every hour up to 4 h. The radioactivity in these aliquots was measured by the addition of 4 ml of scintillation fluid (Ultima Gold; Packard, Meriden, CT) and subsequent liquid scintillation counting (Tri-Carb 2100 CA Liquid Scintillation analyzer; Canberra Packard, Groningen, the Netherlands). Any radioactivity crossing the monolayer and appearing in the opposite compartment was noted as the fraction of total radioactivity added at the beginning of the experiment. Paracellular inulin flux was tolerated up to 2% of the total radioactivity over 4 h.

High-Performance Liquid Chromatography (HPLC) Analysis of Pantoprazole. To determine whether pantoprazole is transported by MRP2 and/or Bcrp1, concentrations of pantoprazole in Optimem medium were measured by use of HPLC analysis. The HPLC system consisted of a P1000 pump and an AS3000 autosampler (Thermo Separation Products, Breda, the Netherlands). Separation was performed using a Zorbax SB-C8 (5 μm; 150 $\times$ 4.6 mm) analytical column (Atas, Zoetermeer, the Netherlands) and a Phenomenex C8 (Octyl, MOS; 4 $\times$ 2 mm) guard column (Bester, Amstelveen, the Netherlands). UV detection was performed using a UV1000 detector (Thermo Separation Products). Retention times and peak areas were analyzed with ChromQuest 2.51 software (Thermo Quest, Breda, the Netherlands). The mobile phase consisted of a mixture of phosphate buffer 5 mM (70% v/v) adjusted to pH 7.0 with 2 M HCl and acetonitril (30% v/v). The flow rate was 1.0 ml/min, and the absorbance was measured at a wavelength of 280 nm. The stock solutions of pantoprazole (Pantozol i.v.) were prepared according to the manufacturer's instructions. Standard samples for calibration were prepared by diluting the stock solution of pantoprazole with Optimem. For the calibration curve, a weighing factor of $1/(\text{concentration})^2$ was used. The calibration curve ranged from 0.5 to 300 μM. All of the samples were injected without additional preparation onto the chromatographic system.

HPLC Analysis of SN38. SN38 concentrations in Optimem medium were determined by HPLC analysis. The chromatographic system consisted of a Waters 616 dual piston pump, a Waters 717 plus autosampler, and a thermostated column compartment. Isocratic elutions were performed using a Chromsep ODS-2 glass column (5 μm; 100 $\times$ 3 mm) and a guard column (Chromsep RP; 5 μm; 10 $\times$ 2 mm). Detection was performed fluorimetrically using a Waters 474 scanning fluorescence detector. Retention times and peak areas were analyzed with Waters Millenium integration software. The mobile phase consisted of a mixture of formic acid 1% (v/v) and acetonitril 17.5% (v/v) adjusted to pH 6.65 with 1 M HCl. The flow rate was 1.0 ml/min, and all of the separations were carried out at 35°C. The excitation and emission settings were 376 and 534 nm, respectively. Preparation of standard solutions of SN38 have been described previously (30). Calibration standards were prepared by dilution of the stock solutions with Optimem medium. The calibration curve for SN38 ranged from 0.01 to 1 μM. Samples were acidified with 0.5 M HCl to maintain SN38 in its lactone form.

Animals. Mice were housed and handled according to institutional guidelines complying with Dutch legislation. Animals used in this study were male *Bcrp1*$^{-/-}$ (*Bcrp1* knockout; Ref. 31) and wild-type mice of a comparable genetic background (FVB or mixed 129/Ola and FVB) between 9 and 14 weeks of age. Animals were kept in a temperature-controlled environment with a 12-h light/12-h dark cycle and received a standard diet (AM-II; Hope Farms, Woerden, the Netherlands) and acidified water *ad libitum*.

Drug Preparation, Administration, and Plasma Analysis. The clinical formulation of MTX (Emthexate) was diluted with NaCl 0.9% to a final concentration of 12.5 mg/ml. A tracer quantity of [^{3}H]MTX was added to the MTX solution. A vial of pantoprazole (Pantozol) was diluted with NaCl 0.9% to a final concentration of 8 mg/ml.

In patients, interactions have been reported between high-dose methotrexate and standard-dose omeprazole, resulting in sustained, highly toxic MTX levels (20, 21). To mimic this interaction in wild-type and *Bcrp1* knockout mice, we calculated the dosage of methotrexate and pantoprazole to be used in mice, as described previously by Freireich *et al.* (32). For MTX, we chose a clinical intermediate high dose of ~250 mg/m^2. For pantoprazole, we also related the standard dose administered to patients (p.o. or i.v. 40–80 mg/day) to the dosage per body surface (*i.e.*, 26–52 mg/m^2). The applied dose in mice (*i.e.*, 120 mg/m^2) was ~2- to 4-fold higher than the clinically applied dose of pantoprazole.

The [^{3}H]MTX was administered i.v. in the tail vein at a dose of 85 mg/kg body weight, which is equivalent to a dose of 255 mg/m^2 MTX (32). Three min before i.v. [^{3}H]MTX, the mice received either i.v. pantoprazole at a dose of 40 mg/kg body weight (*i.e.*, 120 mg/m^2) or i.v. NaCl 0.9% (control) in an equal volume.

Blood samples (30 μl) were taken from the tail vein at 1.5, 3, 10, 30, 60, and 90 min after MTX administration. One hundred twenty minutes after MTX administration, animals were anesthetized with methoxyflurane, their blood was collected by cardiac puncture, and they were sacrificed by cervical dislocation. Coagulation of blood was prevented by use of heparinized capillaries (at time point 1–6) and needle (at last time point) for blood sampling. The plasma fraction of the blood samples was collected after centrifugation at 3000 *g* for 5 min. Radioactivity in plasma samples was determined by liquid scintillation counting (Tri-Carb 2100 CA Liquid Scintillation analyzer; Canberra Packard).

Metabolic Cage Experiment and Statistical Analysis. Mice were housed in a Ruco Type M/1 metabolic cage (Valkenswaard, the Netherlands). They were first accustomed to the cages for 2 days before receiving [^{3}H]MTX (100 mg/kg $\approx$ 300 mg/m^2) injected into the tail vein. Three min before i.v. MTX, the mice received either i.v. pantoprazole (40 mg/kg $\approx$ 120 mg/m^2) or i.v. NaCl 0.9% (control) in an equal volume. Feces and urine were collected in portions of 0–8, 8–24, and 24–48 h after drug administration, and feces was homogenized in 4% (w/v) BSA. Levels of total radioactivity in feces and urine were determined by liquid scintillation counting.

The two-sided unpaired Student's *t* test was used to assess the statistical significance of difference between two sets of data. Each test group was

Downloaded from cancerres.aacrjournals.org on June 8, 2012
Copyright © 2004 American Association for Cancer Research

DOI:10.1158/0008-5472.CAN-03-4062

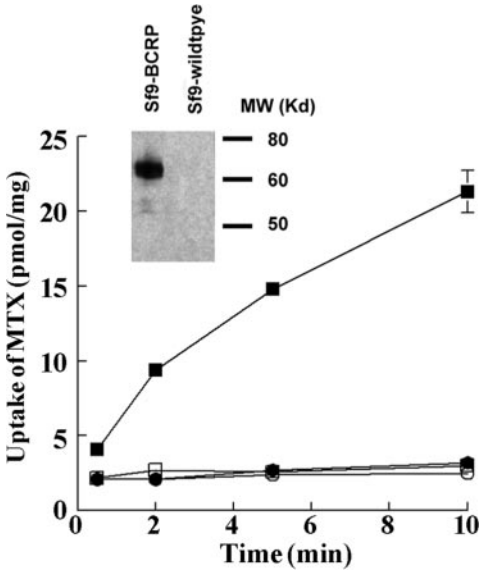

Fig. 1. Time course of ATP-dependent uptake of 1 μM [^{3}H]MTX into membrane vesicles containing BCRP. Membrane vesicles from Sf9 insect cells infected with a BCRP baculovirus (□, ■) and from cells infected with a wild-type baculovirus (○, ●) were incubated at 37°C with 1 μM [^{3}H]MTX for the indicated times in the presence (*closed symbols*) or absence (*open symbols*) of 4 mM ATP. Values shown are of experiments in triplicate. *Inset*, immunoblot analysis of ABCG2 in Sf9 membrane vesicles, which were prepared from Sf9 insect cells transfected with ABCG2-R482 (*Lane 1*) and parental vector (*Lane 2*). Protein (0.5 μg/lane) was size-fractioned on a 7.5% SDS polyacrylamide gel. ABCG2 was detected as described in "Materials and Methods." *Bars*, ±SE.

compared only to the control group. Results are presented as means ± SD. Differences were considered to be statistically significant when $P < 0.05$.

Pharmacokinetic Experiment and Statistical Analysis. Pharmacokinetic parameters after i.v. administration of MTX were calculated according to a two-compartment open model, using the software package MW\Pharm (MEDI\WARE, version 3.02).

The area under the concentration-time curve was calculated using the blood samples collected from the tail vein, *i.e.*, from 0 to 90 min. The area under the concentration-time curve was calculated by the following formula: area under the plasma concentration-time curve = $C_1/\alpha + C_2/\beta$, in which α denotes the exponential rate constant of the initial phase, and β denotes the exponential rate constant of the terminal phase (33). The clearance was calculated by the following formula: clearance = dose/area under the plasma concentration-time curve (AUC). The half-lives of the initial and terminal phase were calculated by the following formula: $t_{1/2}$ (α) = ln2/α and $t_{1/2}$ (β) = ln2/β, respectively (33).

Statistical analyses were performed by ANOVA using Bonferroni post-hoc test for multiple comparisons. Results are presented as the means ± SD. Differences were considered to be statistically significant when $P < 0.05$.

RESULTS

Transport of MTX by BCRP (ABCG2-R482). Membrane vesicles were prepared from Sf9 insect cells transfected with a recombinant baculovirus coding for ABCG2-R482 (BCRP) or with a wild-type baculovirus. Detection with the monoclonal antibody BXP-21 (26) showed that high levels of ABCG2 protein were present in the membranes prepared from transfected Sf9 cells and not in the parental vector-transfected control cells, as indicated by the immunoreactive band of M_r ~70,000 (Fig. 1, inset). MTX is transported by BCRP as shown in Fig. 1, as also demonstrated by Chen *et al.* (12) and Volk *et al.* (13). The initial ATP-dependent uptake rate of 1 μM MTX over the first 2 min was ~3.5 pmol/mg/min in the Sf9-BCRP membrane vesicles and was negligible in the Sf9 wild-type vesicles.

Inhibition of BCRP-Mediated MTX Transport in Sf9 Membrane Vesicles. Using these Sf9-BCRP and Sf9-wild-type membrane vesicles, we studied the effect of different concentrations of pantoprazole and omeprazole on the transport of 1 μM MTX. The ATP-dependent transport of MTX by BCRP was inhibited by the benzimidazoles in a concentration-dependent manner, as shown in Fig. 2, *A* and *B*. IC_{50} values were 13 μM and 36 μM for pantoprazole and omeprazole, respectively.

Stimulation of MRP2 Mediated Transport of MTX in Sf9 Membrane Vesicles. The benzimidazoles did not inhibit the MRP2-mediated transport of MTX in Sf9-MRP2 membrane vesicles. Pantoprazole even stimulated MTX transport in a concentration-dependent manner. At high concentrations of pantoprazole (1 mM), transport of 1 and 100 μM MTX by MRP2 was stimulated 1.6-fold (Fig. 2*C*). This modest stimulation is not unexpected, because we have previously found substantial stimulation of MRP2-mediated transport of $E_2 17\beta G$ by benzimidazoles (27, 34).

Transport of Benzimidazoles by Bcrp1 and not by MRP2 in MDCKII Monolayer. Benzimidazoles have weakly basic properties. At pH 7.4, benzimidazoles (pKa ~ 4) are in an unprotonated form and diffuse readily across intact cells. To determine whether benzimidazoles interfere with drug transport by competition for BCRP, we studied whether pantoprazole is transported by Bcrp1 in MDCKII transfected cells. We also studied whether pantoprazole is transported by MRP2. To exclude any contribution of P-gp, the effective P-gp inhibitors PSC833 (5 μM) and GF120918 (1 μM) were added, respectively, in the MDCKII-*Bcrp1* and MDCKII-*MRP2* cell lines (22, 27, 35). We found transport of pantoprazole by Bcrp1 (Fig. 3) but not by MRP2 (data not shown). This Bcrp1-mediated transport of pantoprazole was saturable, as shown in Fig. 4. The pantoprazole concentration at which half-maximal transport (apparent $K_{1/2}$) of pantoprazole occurred was 0.1–0.2 mM at 4 h transport, but varied from 0.2 to 0.4 mM at t = 2 h and t = 3 h transport of pantoprazole (data not shown).

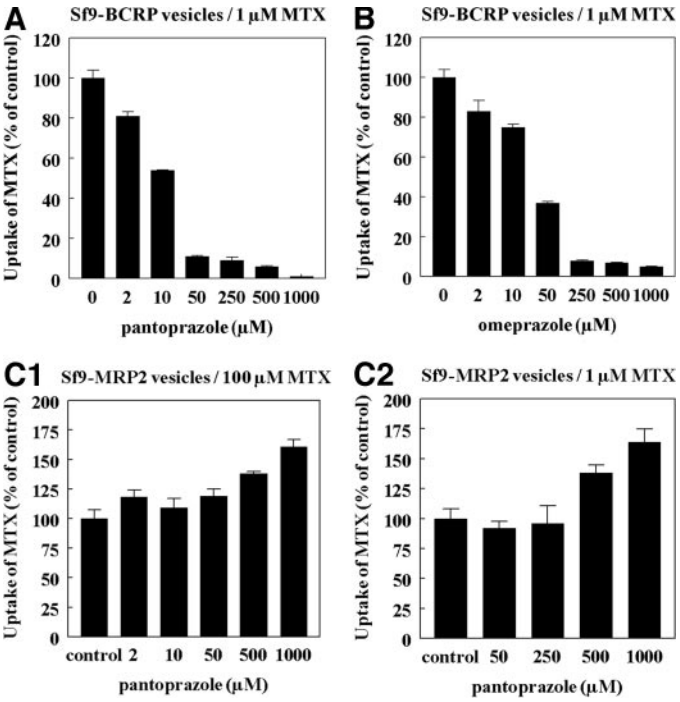

Fig. 2. Effect of pantoprazole and/or omeprazole on ATP-dependent transport of MTX by BCRP and multidrug resistance-associated protein2. Sf9-BCRP membrane vesicles were incubated with 1 μM [^{3}H]MTX for 5 min at 37°C in the presence or absence of pantoprazole (*A*) or omeprazole (*B*). Sf9-multidrug resistance-associated protein2 membrane vesicles were incubated with 1 or 100 μM [^{3}H]MTX for 5 min at 37°C in the presence or absence of pantoprazole (*C1, C2*). The ATP-dependent transport is plotted as percentage of the control value. Values shown are of each experiment in triplicate. *Bars*, ±SE.

Downloaded from cancerres.aacrjournals.org on June 8, 2012
Copyright © 2004 American Association for Cancer Research

DOI:10.1158/0008-5472.CAN-03-4062

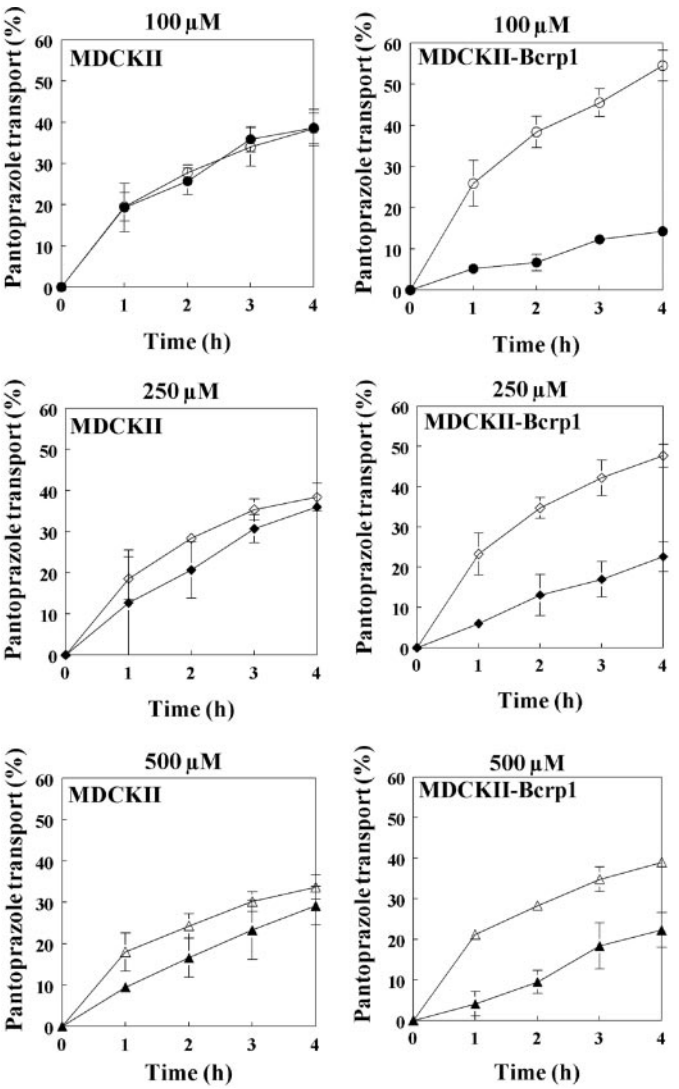

Fig. 3. Transport of pantoprazole by Bcrp1. MDCKII-Parental and MDCKII-Bcrp1 cell lines were preincubated for 2 h with 5 μM PSC833 (in 2 ml Optimem per compartment). The indicated concentration of pantoprazole was applied at t = 0 to the apical or basal side, and the amount of pantoprazole appearing in the opposite basal compartment (*closed symbols*) or apical compartment (*open symbols*) was determined. Samples were taken at t = 1, 2, 3, and 4 h. Values shown are of each experiment in triplicate. *Bars*, ±SD.

Inhibition of Bcrp1-Mediated Transport of Topotecan and SN38 by Pantoprazole. To study the effect of benzimidazoles on the transport of substrate drugs by BCRP, we used 5 μM [^{14}C]topotecan or 1 μM SN38. Both drugs are good model substrates in the MDCKII cell line for BCRP (22, 23). Because topotecan and SN38 are also transported at a low rate by P-gp, the P-gp inhibitor PSC833 (5 μM) was added in these assays to exclude any contribution of P-gp (22, 23, 36). Pantoprazole inhibited the Bcrp1-mediated transport of both drugs, as shown in Fig. 5 for topotecan. Complete inhibition of the Bcrp1-mediated transport of topotecan was reached at a concentration of 500 μM pantoprazole. Transport of SN38 in the *Bcrp1*-transfectant was inhibited 44% by 500 μM pantoprazole and 80% by 1 mM pantoprazole (results not shown). We did not detect transport of topotecan by MRP2, and for SN38, only minimal transport was observed in the MDCKII-MRP2 cell line (data not shown).

Role of Bcrp1 in the Clearance of MTX in Mice. To determine the role of Bcrp1 in the clearance of MTX *in vivo*, we administered i.v. [^{3}H]MTX (85 mg/kg ≈ 255 mg/m^2) to *Bcrp1*$^{+/+}$ (wild-type) and *Bcrp1*$^{-/-}$ (knockout) mice. We measured the MTX plasma concentration by total radioactivity at strategic time-points over a 90-min time period and calculated the pharmacokinetic parameters by a two-compartment pharmacokinetic analysis. The plasma concentration-time curves fitted the applied two-compartment model well ($r^2 \geq 0.99$), which is in line with the pharmacokinetics of MTX described in humans (37). As shown in Fig. 6 and listed in Table 1, the clearance of i.v. MTX was 1.9-fold decreased in *Bcrp1* knockout mice compared with wild-type mice. Although this is highly significant ($P < 0.001$), the half-lives of the initial phase ($t_{1/2}$ α) and the terminal phase ($t_{1/2}$ β) were not significantly different between wild-type and *Bcrp1* knockout mice (Table 1). However, it should be noted that the main differences in plasma disposition of MTX between *Bcrp1* knockout and wild-type mice originated already during the first 5–10 min (Fig. 6). Because the decline of the plasma concentration of MTX was very rapid during the first minutes, the determination of $t_{1/2}$ (α) was inaccurate as shown by the high variation coefficient in $t_{1/2}$ (α). This inaccuracy may mask the expected difference between *Bcrp1* knockout and wild-type mice in $t_{1/2}$ (α). It is obvious, however, that Bcrp1 plays a significant role in the clearance of MTX in mice.

Effect of Pantoprazole on the Bcrp1-Mediated Clearance of MTX in Mice. To investigate whether the interaction between MTX and benzimidazoles, which was observed in cancer patients, is (partly) mediated by BCRP, we determined whether pantoprazole inhibits the Bcrp1-mediated clearance of MTX in mice. We administered i.v. pantoprazole (40 mg/kg ≈ 120 mg/m^2) or i.v. NaCl 0.9% (control) to wild-type mice 3 min before i.v. MTX (85 mg/kg ≈ 255 mg/m^2) and performed plasma pharmacokinetic measurements and model fitting as described previously. The two-compartment model described the observed data well ($r^2 \geq 0.99$). As shown in Fig. 6 and listed in Table 1, coadministration of pantoprazole reduced the clearance of MTX in wild-type mice to the same extent, *i.e.*, 1.8-fold ($P < 0.001$), as observed for the decreased clearance of MTX in the *Bcrp1* knockout mice compared with wild-type mice (1.9-fold). Both the half-life of the initial phase ($t_{1/2}$ α) and the half-life of the terminal phase ($t_{1/2}$ β) were not significantly changed by pantoprazole treatment (Table 1). Also in this situation, however, the variation coefficient in $t_{1/2}$ (α) was high, which may mask the difference between wild-type mice treated with or without pantoprazole.

To determine whether other drug transporters may also play a role in the interaction between benzimidazoles and MTX *in vivo*, we compared the effect of i.v. pantoprazole with the effect of i.v. NaCl 0.9% (control) on the clearance of MTX in *Bcrp1* knockout mice (Fig.

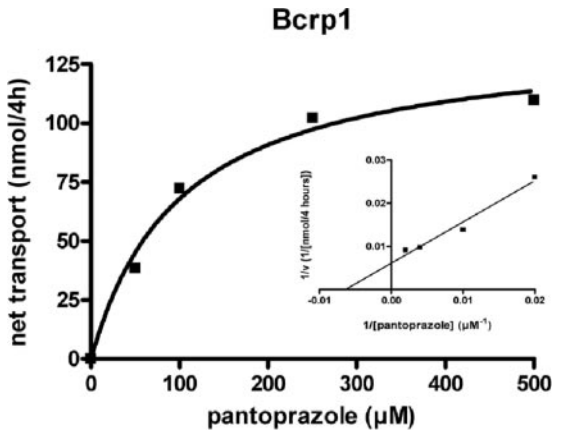

Fig. 4. Saturation kinetics of pantoprazole transport by Bcrp1 in the MDCKII cell line. The difference in transport of pantoprazole in MDCKII-Bcrp1 and MDCKII-Parental cell lines at t = 4 h is plotted against the pantoprazole concentration (in μM). Values shown are means of each experiment in triplicate. *Inset*, Lineweaver-Burk transformation of these results. The apparent $K_{1/2}$ value at t = 4 h is 0.1–0.2 mM.

Downloaded from cancerres.aacrjournals.org on June 8, 2012
Copyright © 2004 American Association for Cancer Research

DOI:10.1158/0008-5472.CAN-03-4062

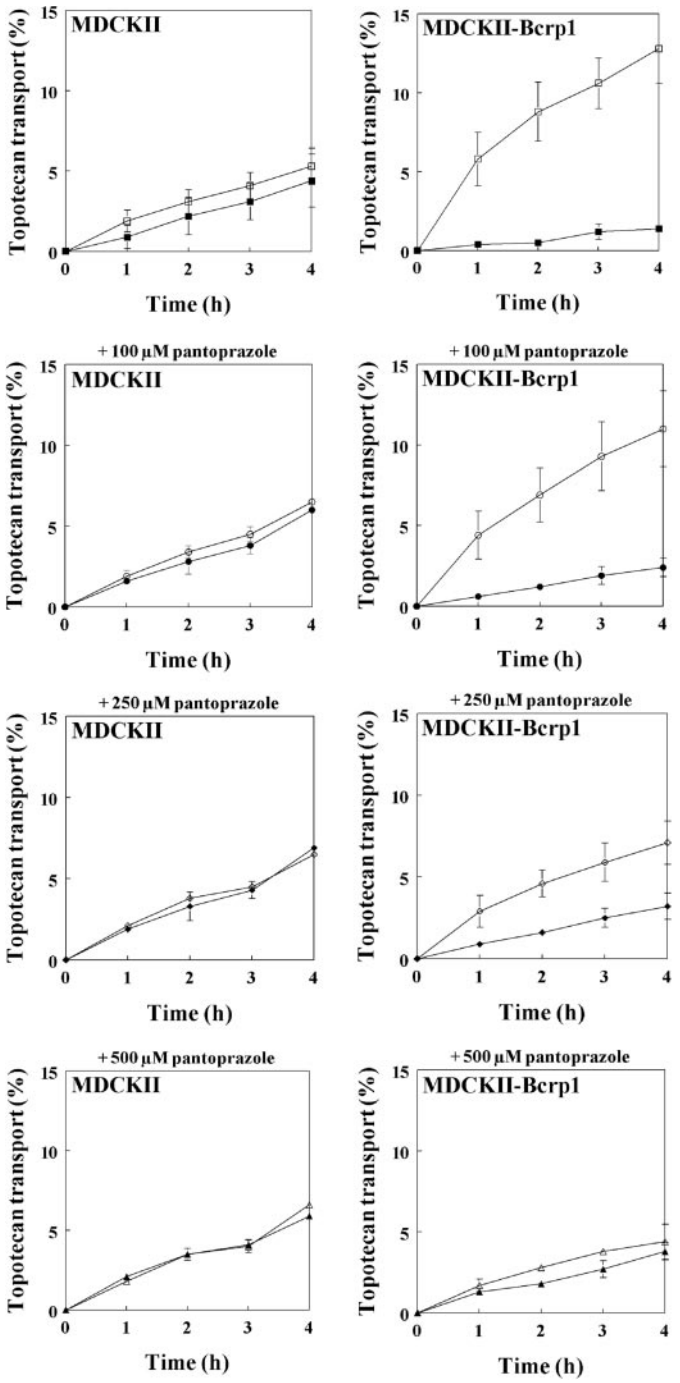

Fig. 5. Transport of 5 μM topotecan by Bcrp1 in the MDCKII cell line in the absence or presence of pantoprazole. The MDCKII-Parental and MDCKII-Bcrp1 cell lines were preincubated for 2 h with 5 μM PSC833 and indicated concentrations of pantoprazole (in 2 ml Optimem per compartment). At t = 0 h, 5 μM topotecan was applied to the apical or basal side, and the amount of topotecan appearing in the opposite basal compartment (*closed symbols*) or apical compartment (*open symbols*) was determined. Samples were taken at t = 1, 2, 3, and 4 h. Values shown are of experiments in triplicate. *Bars*, ±SD.

6; Table 1). The clearance was not significantly different ($P = 0.73$), which suggests that Bcrp1 is the major mediator of the interaction between benzimidazoles and MTX in mice at the dose level of MTX studied.

Fecal and Urinary Excretion of [^{3}H]MTX in Bcrp1 Knockout and Wild-Type Mice. To determine the contribution of Bcrp1 to fecal and urinary excretion of [^{3}H]MTX and the effect of pantoprazole on this, we administered i.v. [^{3}H]MTX (100 mg/kg ≈ 300 mg/m^2) with or without coadministration of i.v. pantoprazole (40 mg/kg ≈ 120 mg/m^2) to *Bcrp1* knockout and wild-type mice and measured fecal and urinary radioactivity. The mice were housed in metabolic cages. Most of the radioactivity in urine and feces was excreted during the first 24 h. In the 24–48 h urine and feces portions, radioactivity was low (~5% additional excretion; data not shown). In wild-type mice, 57 ± 4.4% of the given radioactivity was recovered from feces and 28 ± 2.5% was recovered from urine over the 24 h time-period after administration of [^{3}H]MTX, indicating that fecal excretion is the main excretory pathway for [^{3}H]MTX in mice (Fig. 7). Fecal excretion diminished 1.2-fold in *Bcrp1* knockout mice (46 ± 5.5%; $P < 0.05$), 1.5-fold in wild-type mice pretreated with pantoprazole (37 ± 10%; $P < 0.01$), and 1.6-fold in *Bcrp1* knockout mice pretreated with pantoprazole (36 ± 3.0%; $P < 0.01$) compared with control wild-type mice. However, urinary excretion was not significantly different in *Bcrp1* knockout mice (29 ± 3.7%), in wild-type mice pretreated with pantoprazole (28 ± 8.5%), and in *Bcrp1* knockout mice pretreated with pantoprazole (39 ± 8.5%) compared with control wild-type mice. Together, the data suggest that absence of Bcrp1 or inhibition of Bcrp1 by pantoprazole mainly reduces the fecal excretion and, thus, most likely the hepatic clearance of [^{3}H]MTX in mice.

DISCUSSION

In this study, we show that coadministration of benzimidazoles significantly inhibits BCRP-mediated transport of MTX *in vitro* and reduces the clearance of MTX *in vivo*. *In vitro*, inhibition of BCRP-mediated transport of MTX was reached at clinically relevant concentrations of benzimidazoles (Fig. 2, *A* and *B*). Concentrations of 10 μM pantoprazole or omeprazole resulted in 46% and 25% inhibition of 1 μM MTX, respectively. Standard doses of benzimidazoles in patients give plasma concentrations in the range of 5–10 μM (38). Our *in vitro* results additionally reveal that benzimidazoles are actively transported by Bcrp1 but not by MRP2 (Fig. 3). The Bcrp1-mediated transport of benzimidazoles was saturable (Fig. 4). The observed

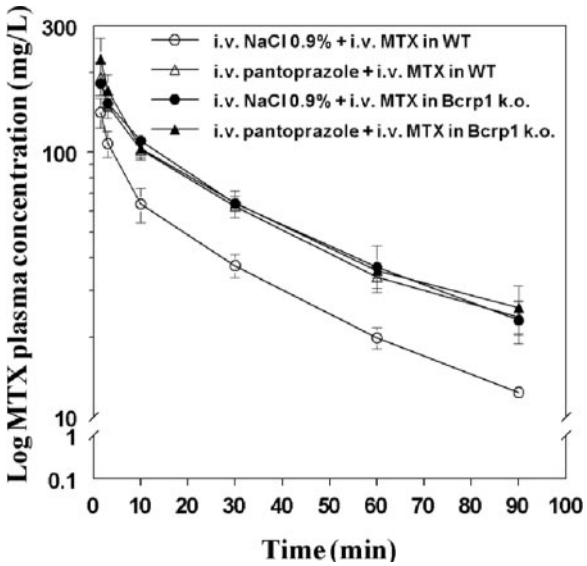

Fig. 6. Semilogarithmic plot of MTX plasma concentration *versus* time curves in mice pretreated with i.v. pantoprazole or i.v. NaCl 0.9% (control). Bcrp1 knockout (*k.o.*) mice (*closed symbols*) or wild-type (*WT*) mice (*open symbols*) were treated with i.v. NaCl 0.9% (*circles*) or i.v. pantoprazole (40 mg/kg ≈ 120 mg/m^2; *triangles*) 3 min before an i.v. dose of MTX (85 mg/kg ≈ 255 mg/m^2). Plasma levels of radiolabeled MTX were determined by liquid scintillation counting at t = 1.5, 3, 10, 30, 60, and 90 min. Results are the means ± SD ($n = 4$). *Bars*, ±SD.

Downloaded from cancerres.aacrjournals.org on June 8, 2012
Copyright © 2004 American Association for Cancer Research

DOI:10.1158/0008-5472.CAN-03-4062

Table 1 *Pharmacokinetic parameters of i.v. [^{3}H]MTX (255 mg/m^2) in wild-type and Bcrp1$^{-/-}$ mice after pretreatment with i.v. pantoprazole (120 mg/m^2) or i.v. NaCl 0.9% (control)*

	Wild-type		Bcrp1$^{-/-}$		Ratio	
	Control + MTX	Pantoprazole + MTX	Control + MTX	Pantoprazole + MTX	Wild-type pantoprazole/control	Bcrp1$^{-/-}$ control/ wild-type control
AUC (h∗mg/L)	57.0 ± 3.81	105 ± 10.0	107 ± 14.5	111 ± 16.9	1.8∗	1.9∗
Cl (L/h/kg)	1.50 ± 0.099	0.815 ± 0.077	0.807 ± 0.105	0.778 ± 0.121	0.54∗	0.54∗
$t_{1/2}$ (α) (h)	0.041 ± 0.014	0.088 ± 0.087	0.094 ± 0.058	0.046 ± 0.012	2.2†	2.3†
$t_{1/2}$ (β) (h)	0.539 ± 0.069	0.775 ± 0.251	0.698 ± 0.144	0.714 ± 0.168	1.4†	1.3†

NOTE. Results are expressed as means ± SD of experiments in quadruplicate.
Abbreviations: AUC, area under the plasma concentration-time curve from 0 to 90 min.; Cl, clearance; $t_{1/2}$ (α), half-life of initial phase; $t_{1/2}$ (β), half-life of terminal phase.
∗ $P < 0.01$.
† $P > 0.05$.

interaction between benzimidazoles and MTX at the level of BCRP is compatible with competitive inhibition of transport. We hypothesized that this competitive inhibition for BCRP may (partly) explain the clinically documented interaction between MTX and benzimidazoles (19, 20, 21). Our *in vivo* data support this assumption. Pantoprazole significantly reduced the clearance of MTX in wild-type mice, and it reduced it to similar levels as in *Bcrp1* knockout mice (Fig. 6). Moreover, in *Bcrp1* knockout mice, the clearance of MTX was not reduced by pantoprazole. Thus, Bcrp1 appears to be the major mediator of the interaction between MTX and benzimidazoles *in vivo* at the dose level of MTX studied.

In humans, the major route of MTX elimination is renal excretion of unmetabolized MTX (39). In rats, 62% of i.v.-administered MTX was excreted into bile, whereas 27% of the dose was excreted into urine, as was shown by Masuda *et al.* (40). This biliary excretion was mediated by MRP2. Furthermore, it was shown in rats that 5.8% of MTX is metabolized by hepatic aldehyde-oxidase to 7-hydroxymethotrexate, which, in turn, is excreted predominantly into the bile as well (41). Henderson *et al.* (42) showed that in mice at a relatively low dose of 15 mg/kg, 60–80% of i.v. [^{3}H]MTX is excreted into the urine, largely within 8 h after injection. However, when [^{3}H]MTX was administered p.o., only 21% appeared in the urine during the 24 h after a 15 mg/kg dose and 37% within 24 h after a 0.5 mg/kg dose. At a dose of 100 mg/kg, we found that 57 ± 4.4% of the i.v.-administered dose of [^{3}H]MTX was excreted in feces and 28 ± 2.5% in urine in wild-type mice. When Bcrp1 was absent or inhibited by pantoprazole, the fecal excretion diminished significantly 1.2- to 1.6-fold. However, the urinary excretion was not significantly different compared with control wild-type mice. This suggests that absence of Bcrp1 or inhibition of Bcrp1 by pantoprazole predominantly affects hepatic clearance of [^{3}H]MTX in mice. The 1.8- to 1.9-fold reduction in plasma clearance of MTX in *Bcrp1* knockout mice and in wild-type mice treated with pantoprazole is most likely caused by reduced hepatobiliary excretion of MTX. In mice, the highest expression of *Bcrp1* mRNA was found in kidney, whereas humans appear to have low renal *BCRP* expression (22, 43, 44). The immunohistochemical studies of Maliepaard *et al.* (26) showed that BCRP was present in the bile canalicular membrane of human liver hepatocytes. Therefore, it is of interest to explore whether in humans pantoprazole exerts its pharmacological effect by affecting the hepatobiliary elimination of (high-dose) MTX.

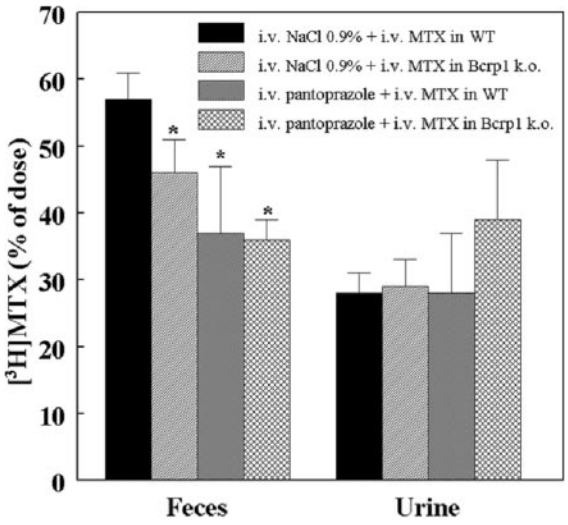

Fig. 7. Fecal and urinary excretion of [^{3}H]MTX in mice pretreated with pantoprazole or NaCl 0.9% (control). Bcrp1 knockout (*k.o.*) mice or wild-type (*WT*) mice were housed in metabolic cages and were treated with i.v. NaCl 0.9% or i.v. pantoprazole (40 mg/kg ≈ 120 mg/m^2) 3 min before an i.v. dose of MTX (100 mg/kg ≈ 300 mg/m^2). Radioactivity was measured in feces and urine excreted between 0–24 h. Results are expressed as percentage of the given dose; *bars*, ±SD ($n = 4$). ∗, $P < 0.05$ compared with wild-type pretreated with control.

We find that the contribution of Bcrp1 to the elimination of MTX (Fig. 6; Table 1) occurs mainly during the first 5 to 10 min after i.v. administration of MTX, when the plasma concentrations of MTX decline rapidly. Thus, the interaction between MTX and pantoprazole seems to take place at high plasma concentrations of MTX. This is plausible because BCRP is a low-affinity, high-capacity transporter of MTX (12, 13). At low concentrations of MTX, other high-affinity transporters, *e.g.*, the reduced folate carrier by which MTX is actively taken up, may be more important in the disposition of MTX (45, 46).

Although we showed that Bcrp1 is the major mediator of the interaction between MTX and benzimidazoles in mice, we cannot exclude that this interaction in patients is also mediated partly by other mechanisms. Reid (20) *et al.* and Beorlegui (21) *et al.* suggested that omeprazole inhibits the H^+,K^+-ATPase in the human kidney, thereby blocking the active tubular secretion of MTX into the urine, resulting in retention of MTX (47). Hitzl (48) *et al.* described recently that patients receiving omeprazole had 4.8-fold higher MRP3 protein levels in the liver. MRP3 is localized in the basolateral membrane of hepatocytes. Up-regulation of MRP3 might, therefore, result in a higher MRP3-mediated efflux of MTX from the liver into the blood circulation rather than into the bile, which might contribute to an increase in plasma concentration of MTX. In our *in vivo* experiments in which pantoprazole was administered 3 min before i.v. MTX, up-regulation of MRP3 is not likely; however, Takeda (18) *et al.* showed that MTX is taken up through the basolateral membrane by hOAT3 and hOAT1 and effluxed through the apical membrane of the proximal tubule via hOAT4. They demonstrated that these hOATs mediated drug interactions between MTX and nonsteroidal anti-inflammatory drugs, probenecid, and penicillin G. Whether hOATs transport benzimidazoles and whether they are involved in the interaction between MTX and benzimidazoles remains to be investigated.

Downloaded from cancerres.aacrjournals.org on June 8, 2012
Copyright © 2004 American Association for Cancer Research

DOI:10.1158/0008-5472.CAN-03-4062

Also, it is not known whether benzimidazoles interfere with cellular uptake of MTX by the reduced folate carrier (45, 46).

Benzimidazoles probably do not interfere with MTX at the level of drug metabolism. Although benzimidazoles are primarily metabolized by CYP2C19 and to a variable extent by CYP3A4 (38, 49), MTX is excreted mostly unchanged, and cytochrome P450 (CYP) enzymes are not involved in MTX metabolism. Approximately 10% of MTX is metabolized by hepatic aldehyde-oxidase to 7-hydroxymethotrexate (39, 41, 42), and whether benzimidazoles interfere with the oxidation of MTX by aldehyde-oxidase is not known. After i.v. administration of MTX, drug-drug interactions may occur because of protein binding displacement and decreased renal clearance of the drug (14–16). Because the plasma protein binding of MTX is only 50%, it seems unlikely that interactions at this level have clinical relevance (50).

In membrane vesicles, we found that pantoprazole inhibited the BCRP-mediated transport of MTX at clinically relevant concentrations (10 μM). Much higher concentrations of pantoprazole appeared to be needed in intact cells to inhibit the Bcrp1-mediated transport of topotecan and SN38 (Fig. 5; data not shown). Topotecan, SN38, and MTX differ in their affinity for BCRP/Bcrp1–topotecan and SN38 having a high affinity (22, 23), and MTX having a low affinity (12, 13). Hence, competition of pantoprazole with topotecan/SN38 for BCRP is probably ineffective, making a clinically relevant pharmacokinetic interaction between pantoprazole and these anticancer agents less likely.

Pauli-Magnus (35) *et al.* described recently that benzimidazoles are substrate drugs of P-gp and inhibit the P-gp-mediated transport of digoxin in Caco-2 cells (IC_{50} values of 17.7 and 17.9 μM for omeprazole and pantoprazole, respectively). We have shown that the low oral bioavailability of substrate drugs for P-gp and BCRP can be improved by oral coadministration of inhibitors of P-gp and/or BCRP, such as cyclosporin A and GF120918 (elacridar; Ref. 22, 51–53). High doses of pantoprazole can be safely applied in humans in the treatment of peptic ulcers (38). Therefore, pantoprazole might be used to improve the oral applicability of P-gp and BCRP substrate drugs, because pantoprazole effectively inhibits BCRP- and P-gp-mediated drug transport. This approach could be explored for MTX despite the interaction between benzimidazoles and MTX at the level of the systemic clearance of MTX. The bioavailability of MTX may be as low as 20% when doses exceed 80 mg/m^2, and these higher doses of MTX are routinely administered i.v. (39). We expect that coadministration of pantoprazole will improve the oral bioavailability of MTX and reduce interpatient variability in systemic exposure to MTX.

Identification of the role of ATP-binding cassette-transporter proteins and/or other transporter systems in drug-drug interactions may help to prevent these interactions and associated toxicities clinically. It is of interest to determine whether BCRP, multidrug resistance-associated protein2, or other ATP-binding cassette-transporters are involved in other clinically important drug-drug interactions with MTX, *e.g.*, nonsteroidal anti-inflammatory drugs, penicillins, ciprofloxacin, cyclosporin A, trimethoprim-sulfamethoxazole, or furosemide (14–18, 54–59). Benzimidazoles are used frequently in the treatment of peptic ulcers, pyrosis, and gastroesophageal reflux disease. This class of drugs is number one on the list of most prescribed drugs worldwide. It is of interest for the clinic, therefore, to explore whether BCRP, multidrug resistance-associated protein2, and/or P-gp are involved in other known drug-drug interactions with benzimidazoles, *e.g.*, in combination with triazoles (itraconazole, ketoconazole, voriconazole), phenytoin, or diazepam (60, 61).

In conclusion, benzimidazoles represent a new class of drugs that differentially affect BCRP- and multidrug resistance-associated protein2-mediated transport of MTX. Competition for BCRP may explain the pharmacokinetic interaction between MTX and benzimidazoles observed in patients.

ACKNOWLEDGMENTS

We are grateful to Maarten Huisman (Division of Experimental Therapy, The Netherlands Cancer Institute, Amsterdam, the Netherlands) for technical advice and support, and we thank Rianne van Maanen (Department of Pharmacy and Pharmacology, Slotervaart Hospital, Amsterdam, the Netherlands), Annemieke Kuil (Division of Molecular Biology, The Netherlands Cancer Institute, Amsterdam, the Netherlands), and Greta Cipriani (Division of Experimental Therapy, The Netherlands Cancer Institute, Amsterdam, the Netherlands) for technical assistance, Puck Knipscheer and Joyce Lebbink (Division of Molecular Carcinogenesis, The Netherlands Cancer Institute, Amsterdam, the Netherlands) for providing us with Sf9 insect cells, Els Wagenaar (Division of Experimental Therapy, The Netherlands Cancer Institute, Amsterdam, the Netherlands) for providing us with mice, and Balazs Sarkadi (National Institute of Hematology) for providing us with recombinant baculoviruses coding for BCRP and MRP2.

REFERENCES

1. Alt FW, Kellems RE, Bertino JR, Schimke RT. Selective multiplication of dihydrofolate reductase genes in methotrexate-resistant variants of cultured murine cells. J Biol Chem 1978;253:1357–70.
2. Dicker AP, Volkenandt M, Schweitzer BI, Banerjee D, Bertino JR. Identification and characterization of a mutation in the dihydrofolate reductase gene from the methotrexate-resistant Chinese hamster ovary cell line Pro-3 MtxRIII. J Biol Chem 1990; 265:8317–21.
3. Yu M, Melera PW. Allelic variation in the dihydrofolate reductase gene at amino acid position 95 contributes to antifolate resistance in Chinese hamster cells. Cancer Res 1993;53:6031–5.
4. Srimatkandada S, Schweitzer BI, Moroson BA, Dube S, Bertino JR. Amplification of a polymorphic dihydrofolate reductase gene expressing an enzyme with decreased binding to methotrexate in a human colon carcinoma cell line, HCT-8R4, resistant to this drug. J Biol Chem 1989;264:3524–8.
5. Hooijberg JH, Broxterman HJ, Kool M, et al. Antifolate resistance mediated by the multidrug resistance proteins MRP1 and MRP2. Cancer Res 1999;59:2532–5.
6. Kool M, van der Linden M, de Haas M, et al. MRP3, an organic anion transporter able to transport anti-cancer drugs. Proc Natl Acad Sci USA 1999;96:6914–9.
7. Bakos E, Evers R, Sinko E, et al. Interactions of the human multidrug resistance proteins MRP1 and MRP2 with organic anions. Mol Pharmacol 2000;57:760–8.
8. Zeng H, Chen ZS, Belinsky MG, Rea PA, Kruh GD. Transport of methotrexate (MTX) and folates by multidrug resistance protein (MRP) 3 and MRP1: effect of polyglutamylation on MTX transport. Cancer Res 2001;61:7225–32.
9. Chen ZS, Lee K, Walther S, et al. Analysis of methotrexate and folate transport by multidrug resistance protein 4 (ABCC4): MRP4 is a component of the methotrexate efflux system. Cancer Res 2002;62:3144–50.
10. Volk EL, Farley KM, Wu Y, et al. Overexpression of wild-type breast cancer resistance protein mediates methotrexate resistance. Cancer Res 2002;62:5035–40.
11. Volk EL, Rohde K, Rhee M, et al. Methotrexate cross-resistance in a mitoxantrone-selected multidrug-resistant MCF7 breast cancer cell line is attributable to enhanced energy-dependent drug efflux. Cancer Res 2000;60:3514–21.
12. Chen ZS, Robey RW, Belinsky MG, et al. Transport of methotrexate, methotrexate polyglutamates, and 17beta-estradiol 17-(beta-D-glucuronide) by ABCG2: effects of acquired mutations at R482 on methotrexate transport. Cancer Res 2003;63:4048–54.
13. Volk EL, Schneider E. Wild-type breast cancer resistance protein (BCRP/ABCG2) is a methotrexate polyglutamate transporter. Cancer Res 2003;63:5538–43.
14. Ellison NM, Servi RJ. Acute renal failure and death following sequential intermediate-dose methotrexate and 5-FU: a possible adverse effect due to concomitant indomethacin administration. Cancer Treat Rep 1985;69:342–3.
15. Thyss A, Milano G, Kubar J, Namer M, Schneider M. Clinical and pharmacokinetic evidence of a life-threatening interaction between methotrexate and ketoprofen. Lancet 1986;1:256–8.
16. Tracy TS, Krohn K, Jones DR, et al. The effects of a salicylate, ibuprofen, and naproxen on the disposition of methotrexate in patients with rheumatoid arthritis. Eur J Clin Pharmacol 1992;42:121–5.
17. Kremer JM, Hamilton RA. The effects of nonsteroidal antiinflammatory drugs on methotrexate (MTX) pharmacokinetics: impairment of renal clearance of MTX at weekly maintenance doses but not at 7.5 mg. J Rheumatol 1995;22:2072–7.
18. Takeda M, Khamdang S, Narikawa S, et al. Characterization of methotrexate transport and its drug interactions with human organic anion transporters. J Pharmacol Exp Ther 2002;302:666–71.
19. Tröger U, Stotzel B, Martens-Lobenhoffer J, Gollnick H, Meyer FP. Drug points: severe myalgia from an interaction between treatments with pantoprazole and methotrexate. BMJ 2002;324:1497.
20. Reid T, Yuen A, Catolico M, Carlson RW. Impact of omeprazole on the plasma clearance of methotrexate. Cancer Chemother Pharmacol 1993;33:82–4.
21. Beorlegui B, Aldaz A, Ortega A, et al. Potential interaction between methotrexate and omeprazole. Ann Pharmacother 2000;34:1024–7.

Downloaded from cancerres.aacrjournals.org on June 8, 2012
Copyright © 2004 American Association for Cancer Research

DOI:10.1158/0008-5472.CAN-03-4062

22. Jonker JW, Smit JW, Brinkhuis RF, et al. Role of breast cancer resistance protein in the bioavailability and fetal penetration of topotecan. J Natl Cancer Inst (Bethesda) 2000;92:1651–6.
23. Nakatomi K, Yoshikawa M, Oka M, et al. Transport of 7-ethyl-10-hydroxycamptothecin (SN-38) by breast cancer resistance protein ABCG2 in human lung cancer cells. Biochem Biophys Res Commun 2001;288:827–32.
24. Louvard D. Apical membrane aminopeptidase appears at site of cell-cell contact in cultured kidney epithelial cells. Proc Natl Acad Sci USA 1980;77:4132–6.
25. Evers R, Kool M, van Deemter L, et al. Drug export activity of the human canalicular multispecific organic anion transporter in polarized kidney MDCK cells expressing cMOAT (MRP2) cDNA. J Clin Investig 1998;101:1310–9.
26. Maliepaard M, Scheffer GL, Faneyte IF, et al. Subcellular localization and distribution of the breast cancer resistance protein transporter in normal human tissues. Cancer Res 2001;61:3458–64.
27. Zelcer N, Huisman MT, Reid G, et al. Evidence for two interacting ligand-binding sites in human MRP2 (ABCC2). J Biol Chem 2003;278:23538–44.
28. Heijn M, Hooijberg JH, Scheffer GL, et al. Anthracyclines modulate multidrug resistance protein (MRP) mediated organic anion transport. Biochim Biophys Acta 1997;1326:12–22.
29. Zelcer N, Saeki T, Reid G, Beijnen JH, Borst P. Characterization of drug transport by the human multidrug resistance protein 3 (ABCC3). J Biol Chem 2001;276:46400–7.
30. Schoemaker NE, Rosing H, Jansen S, Schellens JH, Beijnen JH. High-performance liquid chromatographic analysis of the anticancer drug irinotecan (CPT-11) and its active metabolite SN-38 in human plasma. Ther Drug Monit 2003;25:120–4.
31. Jonker JW, Buitelaar M, Wagenaar E, et al. The breast cancer resistance protein protects against a major chlorophyll-derived dietary phototoxin and protoporphyria. Proc Natl Acad Sci USA 2002;99:15649–54.
32. Freireich EJ, Gehan EA, Rall DP, Schmidt LH, Skipper HE. Quantitative comparison of toxicity of anticancer agents in mouse, rat, hamster, dog, monkey, and man. Cancer Chemother Rep 1966;50:219–44.
33. Rowland M, Tozer TN. Clinical pharmacokinetics. Concepts and applications. 3rd ed. Chapter 19, Distribution kinetics. Philadelphia: Lippincott Williams & Wilkins; 1995. p. 313–39.
34. Breedveld P, Zelcer N, Pluim D, et al. Benzimidazoles inhibit BCRP (ABCG2)- and P-gp (ABCB1)-mediated drug transport and potentiate MRP2 (ABCC2)-mediated drug transport [abstract]. 2nd ed. Proc Am Assoc Cancer Res. 2003;44:R599.
35. Pauli-Magnus C, Rekersbrink S, Klotz U, Fromm MF. Interaction of omeprazole, lansoprazole and pantoprazole with P-glycoprotein. Naunyn Schmiedebergs Arch Pharmacol 2001;364:551–7.
36. Chu XY, Suzuki H, Ueda K, et al. Active efflux of CPT-11 and its metabolites in human KB-derived cell lines. J Pharmacol Exp Ther 1999;288:735–41.
37. Sabot C, Debord J, Roullet B, et al. Comparison of 2- and 3-compartment models for the Bayesian estimation of methotrexate pharmacokinetics. Int J Clin Pharmacol Ther 1995;33:164–9.
38. Huber R, Hartmann M, Bliesath H, et al. Pharmacokinetics of pantoprazole in man. Int J Clin Pharmacol Ther 1996;34:S7–16.
39. Hardman JG, Limbird LE, Gilman AG. Goodman & Gilman's the pharmacological basis of therapeutics. 10th ed. Chapter 52, Antineoplastic agents. New York: McGraw-Hill; 2001. p. 1399–404.
40. Masuda M, I'izuka Y, Yamazaki M, et al. Methotrexate is excreted into the bile by canalicular multispecific organic anion transporter in rats. Cancer Res 1997;57:3506–10.
41. Fahrig L, Brasch H, Iven H. Pharmacokinetics of methotrexate (MTX) and 7-hydroxymethotrexate (7-OH-MTX) in rats and evidence for the metabolism of MTX to 7-OH-MTX. Cancer Chemother Pharmacol 1989;23:156–60.
42. Henderson ES, Adamson RH, Denham C, Oliverio VT. The metabolic fate of tritiated methotrexate. I. Absorption, excretion, and distribution in mice, rats, dogs and monkeys Cancer Res 1965;25:1008–17.
43. Doyle LA, Yang W, Abruzzo LV, et al. A multidrug resistance transporter from human MCF-7 breast cancer cells. Proc Natl Acad Sci USA 1998;95:15665–70.
44. Allikmets R, Schriml LM, Hutchinson A, Romano-Spica V, Dean M. A human placenta-specific ATP-binding cassette gene (ABCP) on chromosome 4q22 that is involved in multidrug resistance. Cancer Res 1998;58:5337–9.
45. Ulrich CM, Robien K, Sparks R. Pharmacogenetics and folate metabolism–a promising direction. Pharmacogenomics 2002;3:299–313.
46. Westerhof GR, Rijnboutt S, Schornagel JH, et al. Functional activity of the reduced folate carrier in KB, MA104, and IGROV-I cells expressing folate-binding protein. Cancer Res 1995;55:3795–802.
47. Kraut JA, Starr F, Sachs G, Reuben M. Expression of gastric and colonic H(+)-K(+)-ATPase in the rat kidney. Am J Physiol 1995;268:F581–7.
48. Hitzl M, Klein K, Zanger UM, et al. Influence of omeprazole on multidrug resistance protein 3 expression in human liver. J Pharmacol Exp Ther 2003;304:524–30.
49. Andersson T. Pharmacokinetics, metabolism and interactions of acid pump inhibitors. Focus on omeprazole, lansoprazole and pantoprazole. Clin Pharmacokinet 1996;31:9–28.
50. Benet LZ, Hoener BA. Changes in plasma protein binding have little clinical relevance. Clin Pharmacol Ther 2002;71:115–21.
51. Bardelmeijer HA, Beijnen JH, Brouwer KR, et al. Increased oral bioavailability of paclitaxel by GF120918 in mice through selective modulation of P-glycoprotein. Clin Cancer Res 2000;6:4416–21.
52. Meerum Terwogt JM, Malingré MM, Beijnen JH, et al. Coadministration of oral cyclosporin A enables oral therapy with paclitaxel. Clin Cancer Res 1999;5:3379–84.
53. Malingré MM, Beijnen JH, Rosing H, et al. Co-administration of GF120918 significantly increases the systemic exposure to oral paclitaxel in cancer patients. Br J Cancer 2001;84:42–7.
54. Najjar TA, Abou-Auda HS, Ghilzai NM. Influence of piperacillin on the pharmacokinetics of methotrexate and 7- hydroxymethotrexate. Cancer Chemother Pharmacol 1998;42:423–8.
55. Titier K, Lagrange F, Pehourcq F, Moore N, Molimard M. Pharmacokinetic interaction between high-dose methotrexate and oxacillin. Ther Drug Monit 2002;24:570–2.
56. Dalle JH, Auvrignon A, Vassal G, Leverger G. Interaction between methotrexate and ciprofloxacin. J Pediatr Hematol Oncol 2002;24:321–2.
57. Fox RI, Morgan SL, Smith HT, et al. Combined oral cyclosporin and methotrexate therapy in patients with rheumatoid arthritis elevates methotrexate levels and reduces 7-hydroxymethotrexate levels when compared with methotrexate alone. Rheumatology (Oxford) 2003;48:989–94.
58. Groenendal H, Rampen FH. Methotrexate and trimethoprim-sulphamethoxazole–a potentially hazardous combination. Clin Exp Dermatol 1990;15:358–60.
59. Nierenberg DW, Mamelok RD. Toxic reaction to methotrexate in a patient receiving penicillin and furosemide: a possible interaction. Arch Dermatol 1983;119:449–50.
60. Stockley ID. Drug interactions. 4th ed. London: The Pharmaceutical Press; 1996. p. 147–8.
61. Desta Z, Zhao X, Shin JG, Flockhart DA. Clinical significance of the cytochrome P450 2C19 genetic polymorphism. Clin Pharmacokinet 2002;41:913–58.

Downloaded from cancerres.aacrjournals.org on June 8, 2012
Copyright © 2004 American Association for Cancer Research